Journal of Applied Sciences

ISSN 1812-5654

science alert

ANSInet
an open access publisher
http://ansinet.com

Journal of Applied Sciences 12 (21): 2235-2243, 2012
ISSN 1812-5654 / DOI: 10.3923/jas.2012.2235.2243

Mapping Full-field Bond Stress Distribution on Concrete using Digital Image Correlation Results

[1]Reza Aghlara, [2]Redzuan Abdullah and [2]Mahmood Md. Tahir
[1]Department of Civil Engineering, Ahar Branch, Islamic Azad University, Ahar, Iran
[2]Department of Structures and Materials, Faculty of Civil Engineering,
Universiti Teknologi Malaysia, Johor, Malaysia

Abstract: A pull-out concrete specimen was subjected to tensile load in order to obtain the bond stress distribution on its surface using the results of Two Dimensional Digital Image Correlation (2D DIC). Digital images were taken from front face of specimen by a typical digital camera (Nikon D80) and used as input data of correlation software for strain analysis. The correctness of analysis results were controlled by results of linear variable differential transformer instrument LVDT which it was installed by specimen in the experiment. After obtaining bond strain components on the face of specimen, the related bond stress components were calculated numerically with considering the specimen face as plain stress. The results show high capability of used method and technique for investigation on bond in concrete.

Key words: Concrete, bond stress, pull-out test, 2D digital image correlation

INTRODUCTION

Two Dimensional Image Correlation (2D DIC) is now broadly recognised and applied in the most experimental fields as a practical and capable instrument for in-plane deformation measurement of a planar object surface. The full-field displacements and strains to sub-pixel accuracy are calculated directly by comparing the digital images of a test object acquired before and after deformation (Pan *et al*., 2009a). On the other side, the importance of the material as reinforced concrete in the structures is known to everyone who is involved in construction. So, it seems that every property of this material will have a great importance to study extensively by the new techniques in order to discover precise behaviour of that material perfectly. One of the most important feature in the reinforced concrete is the bond between bars and concrete that was studied in this project. The joint performance of steel and concrete in a reinforced concrete element is based on the fact that a bond is maintained between two materials after concrete hardens. The bond strength depends on three major factors, as friction between steel and concrete, interlocking and chemical adhesion (Nadim Hasson and Al-Manaseer, 2008).

Theoretically, the calculated bond strength depends on several effective factors and it has not completely equaled with practical results (Vandewalle and Mortelmans, 1988). In order to have a useful step and dependable criteria to judge theoretical results, realistic bond stress distribution based on experimental sample seems to be helpful to great extent. Furthermore, such approaches can help us to gain enhanced understanding of bond behavior that may lead to appropriate usage of bars in concrete structures. Accordingly, it may change some related conception or may help in discoveries innovative ideas in the bond field.

As shown in Fig. 1, the reactions of subjected tensile force to the reinforcement in concrete block are inclined reaction forces (Fig. 1a) that can be presented with two components (Fig. 1b), parallel and normal to the bar axes (Nadim Hasson and Al-Manaseer, 2008). The main purposes of this investigation were calculation of the bond stress components and mapping the distribution of them on the concrete.

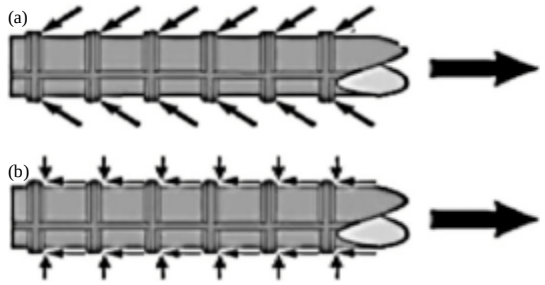

Fig. 1(a-b): (a) Subjected tensile force and inclined reaction forces and (b) Subjected tensile force and two components of reaction forces

Corresponding Author: Reza Aghlara, Department of Civil Engineering, Ahar Branch, Islamic Azad University, Ahar, Iran

TWO DIMENSIONAL DIGITAL IMAGE CORRELATION

Overview: One of the important tasks of experimental solid mechanics is the measurement of the surface deformation and motion of material which is subjected to various loadings. Apart from the commonly used conventional tool for test measurement; such as LVDT, strain gauges, extensometer and etc., several full-field non-contact optical methods have been developed and applied for this purpose. The method of 2D DIC, developed at the University of South Carolina in 1980s, is one of the non-contact optical technique that is widely accepted and used as a powerful tool for the surface measurement (Peter and Ranson, 1982). This method uses a single fix camera and is limited to in-plane deformation measurement of the planar object surface. In this technique, the full-field displacement and strain are measured by comparing grey intensity changes of digital images of the specimen surface in un-deformed and deformed states respectively (Sutton *et al*., 1986).

The advantage of the DIC method is that the experimental setup and specimen preparation are quite simple (Schreier, 2003). For recording the digital images of specimen before and after deformation, only one fixed CCD camera is needed. A white light source or natural light can be used for illumination during loading. On the weakness side, the object surface to be measured must be planar and must have a random grey intensity. Besides, the use of high quality imaging system is very important because the image quality has a considerable effect on reliability of measurement. Some developments in DIC; such as reduction of computation complexity and accomplishing high accuracy deformation measurement, has been widely explored and considerably improved in recent years (Sutton *et al*., 2008).

Fundamentals of 2D DIC: In this experimental a typical digital image camera (Nikon D80) for acquiring images of test specimen is applied as shown in Fig. 2. A computer is connected to this CCD camera in order to control and take images automatically on regular bases. The camera is adjusted with normal optical axis to the specimen surface. This surface which is illuminated by white light sources, must have a random gray intensity distribution (i.e., speckle pattern). This feature deforms together with the object surface as a carrier of deformation information. The speckle pattern can be the natural texture of the surface or artificially made by spraying black and white paints.

The actual physical motion of one point on the specimen surface is calculated by the estimated motion of image point multiplying the magnification of the imaging

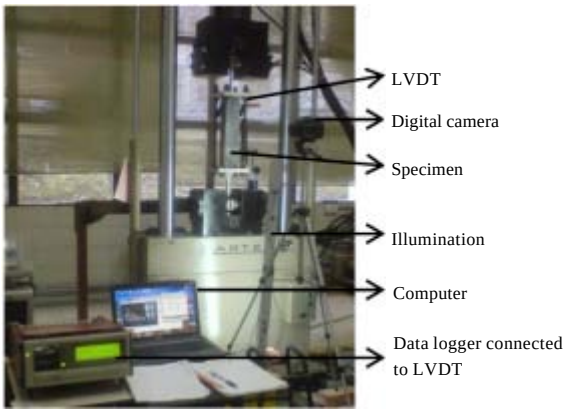

Fig. 2: 2D DIC experimental system in the research

system (in units of mm/pixel). In order to obtain good result, the object surface must be flat and remain in the same plane parallel to the CCD sensor camera during the loading. Any out-of-plane motion will change the magnification of the recorded images and this will lead to some error in calculation of displacement. Minimizing this error effect, use of telecentric imaging system or placing the camera far from the specimen is proposed (Sutton *et al*., 2008). Secondly, geometric distortion in imaging system could produce some errors in calculation of displacement. It is important that this error is reduced to minimal level. However, techniques for correction of the geometric distortion are available (Pan *et al*., 2009b).

The motion of each point at image is calculated by comparing the digital images taken during test, using DIC software. Generally, several software are available for correlation in market as RapidCorrelator, Vic 2D, Opticist and MATLAB toolbox. At the first step of 2D DIC method, the Region of Interest (ROI) should be defined on the reference image. This area will be divided into evenly spaced virtual grids. Calculation of full-field deformation will be done based on the obtained displacement of each grid points. For this purpose, small equal square area as subsets are assigned to every grid point in some way that the point locates in the centre of square (Fig. 3). The subsets have specific number of points and their value in grey level, so for every subset in estimated deformed shape, a criterion as Cross-correlation (CC) or Sum-squared Difference (SSD) can be calculated. Having the distribution of these criterions and choosing the peak value can yield to the desire deformed subset. Therefore, with this method each subset could be traced in the next image. These related subset and its centre, leads to the new location of the correlated points in the deformed images. The differences in centres of reference and target

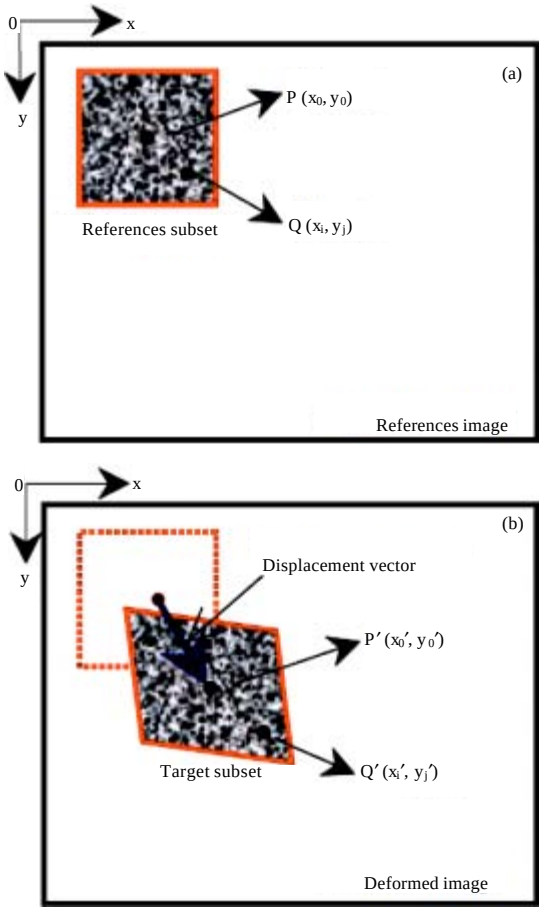

Fig. 3(a-b): Schematic illustration of a reference square subset (a) Before and (b) After deformation (Pan *et al*., 2009b)

subsets yield in-plane displacement vector at two centre points. This process will be continued till all the grid points' displacements are obtained.

Then, the new location of the rest points in the deformed subset can be computed by using a math formula termed as shape function. This function is obtained easily by using the data of the primary achieved displacement vector of subsets center. A zero-order function can be used when the subsets displacement in reference and deformed images is occurred because of only the rigid body translation. A first-order shape function can be applied when translation, rotation and their combination exist in deformed subset.

In calculation of the other points coordinate in the subset by using the shape function, there is a probability that the coordinate of new point would be located between two points. Solving this issue, a certain sub-pixel interpolation scheme should be employed to provide the location of these points with the intensity, before using correlation criterion or evaluating the similarity of subsets. Miscellaneous interpolation schemes are used in literature and their detailed algorithms can be found in numerical computing books (William, 2003). Nevertheless, bicubic and biquintic spline interpolation as a higher-order interpolation scheme is greatly suggested by Knauss *et al*. (2003).

Displacement and strain field measurement: The integer displacements with one pixel accuracy are computed easily because of the distinct nature of digital images. Certain sub-pixel registration algorithms should be applied for having more accuracy in this measurement (Bing *et al*., 2006). Therefore, to achieve this level of accuracy two following steps, namely initial deformation estimation and sub-pixel displacement measurement should have been considered in the implementation of 2D DIC. This means that for having sub-pixel accuracy in 2D DIC method, an accurate initial guess of the deformation should be employed primarily. Strain distribution is more desirable in most measurement area in the theory and practice. The strain is calculated from the results of displacement. Pan and Xie (2009) discussed the methods for calculating strain.

Errors in 2D DIC measurement: 2D DIC is heavily depending on the quality of loading system, the perfection of imaging system and the accuracy of correlation algorithms. The measurement in higher level of accuracy relies directly to the estimation of the errors and their sources (Haddadi and Belhabib, 2008). Entirely, the error sources can be divided into two discrete categories, namely errors during test and errors after the test. The first group which is related to the specimen, loading and imaging consists of four major elements, specifically speckles pattern, test object position, image distortions and noises. The second group is related to the correlation algorithm composed of fours features, called subset size, correlation criteria, interpolation scheme and shape function (Pan and Xie, 2009).

Application of 2D DIC: A large number of applications of 2D DIC are available in the literature. Some of the important ones can be listed as, determining the deformation field of various materials subjected to loading, determining the different mechanical parameters of a material including Young's modulus, Poisson's ratio, stress intensity factor, residual stress and thermal expansion coefficient and the elastic properties of materials. Numerous other interesting applications can be found in the experimental works based on measurement using DIC. Valenca *et al*. (2012) has introduced an innovative method named MCRACK to characterise

cracks automatically using processing of digital images. This interesting method, in spite of reducing working time significantly, gives a considerable increase of data, with higher reliability in cracks. Rouchier (2012) proposed digital image correlation as a suitable method to obtain complete mapping of the deformations at the surface of the samples and the use of non-destructive fracture characterization for the purpose of moisture transfer modelling. In the field of damage assessment in the Reinforced Concrete (RC), the combination of DIC method and acoustic emission technique have used to provide the state of damage in RC structures (Vidya Sagar and Raghu Prasad, 2012). Gardner has showed DIC can be suitable for measuring the deflections of the masonry wall panels in an experiment (Herbert *et al*., 2011).

EXPERIMENTAL PROCEDURES

The experiment is done with image acquiring of the concrete block surface during the pull out test. A concrete block (400×100×55 mm) with embedded steel bar (⌀12) was prepared with the mix proportion of cement, water, fine and coarse aggregate of 410, 250, 997 and 693 kg for producing one cubic meter of concrete. The specimen was cured in room temperature for 28 days before conducting the pull out test. The concrete compressive strength tested at 28 days was 31 MPa. Before conducting the pull out test, the specimen surface was coated with white and black paint in order to have proper speckle pattern with high contrast. Once the specimen was secured on the test bed, a CCD digital camera was setup on a leveled tripod. The camera was located and adjusted such that the lens axes was directed perpendicular to the side surface of the concrete block to be recorded. The camera was connected to a computer and the snapping was controlled and done automatically by software. An LVDT was installed next to the specimen to record the displacement of a point that is shown in Fig. 4. Pull out load was applied to the bar using Universal Machine at the speed of 0.05 kN sec^{-1} until failure. The images of the concrete block surface were taken at every two seconds during loading. The LVDT reading was taken at every 10 sec during loading. The pull out specimen set up is shown in Fig. 4. The obtained digital images were used as input data for correlation software to analyze the displacement and strain of the concrete surface.

RESULTS AND DISCUSSION

Controlling the correctness of DIC result: Displacements of a specific point on the specimen (Fig. 4), calculated by two different correlation software, are compared with LVDT recorded results in Fig. 5. The

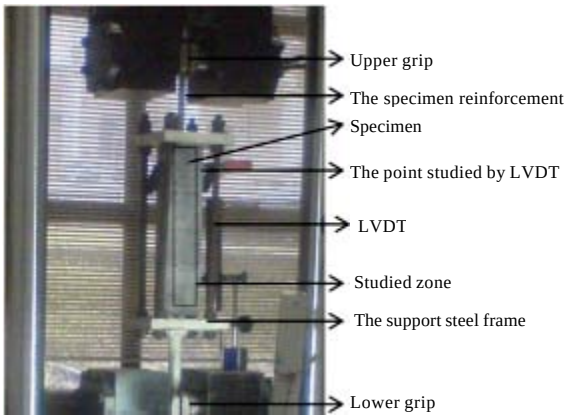

Fig. 4: Specimen set up in pullout test

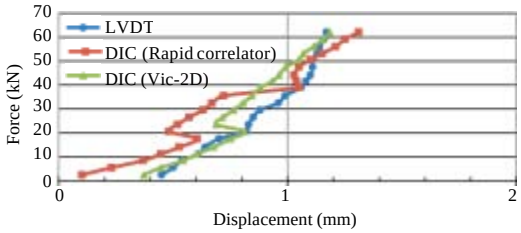

Fig. 5: Load versus displacement of the certain point

trends of two displacement curves obtained from DIC software are almost same. However, there is a little difference in quantities of displacements. which, the reason can be the use of dissimilar algorithm or correlation criterion. In the following, the results of Vic-2D are used for further analysis and discussion.

Strain distribution: Having detailed assessment for better investigation, the numerical results of correlation software are used for mapping full-field distribution of three principal components of bond strain on the surface of the specimen by Excel in Fig. 6a, when the tensile force is 67 kN.

In Fig. 6b, the major principal strain distribution, the effect of bond action between concrete and reinforcement on the strain distribution is observed clearly. The sharp increase of strain on the top of the bar is because of the existence of the bond between concrete and reinforcement. The minor principal strain distribution, Fig. 6c, manifests that the bond has influence around the bar but with less intensity in comparison with the principal strain distribution. As a remarkable point, it is obviously seen that this component of strain has negative quantities in the most part of the specimen surface. Last chart, Fig. 6d which illustrates the principal strain angel distribution, exhibits that this strain in the specimen sides,

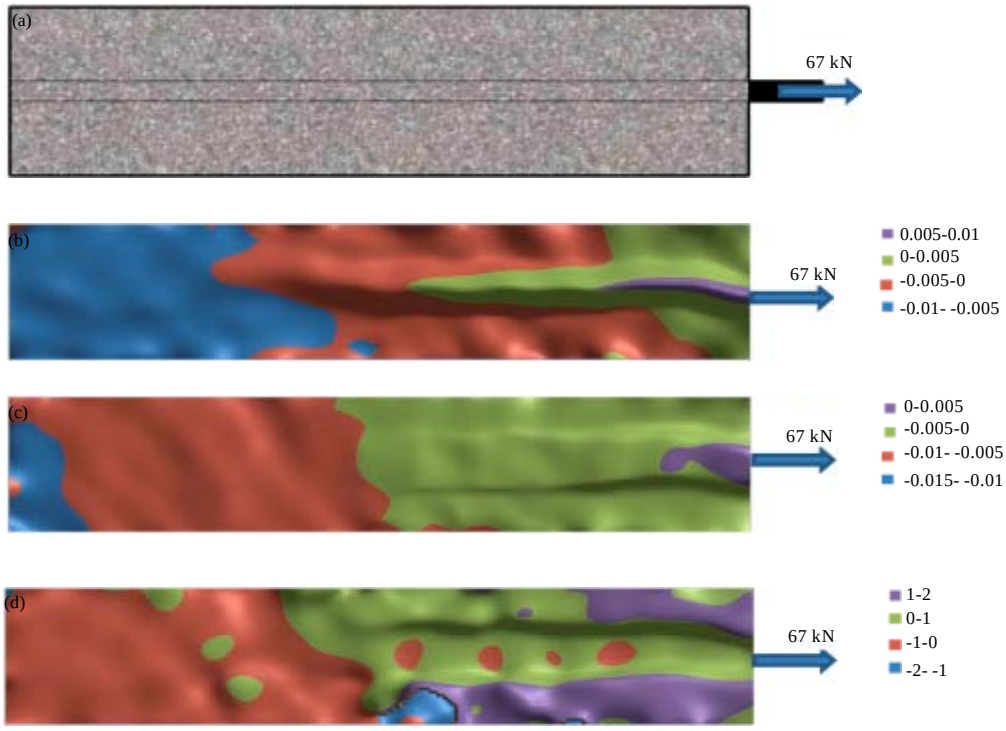

Fig. 6(a-d): (a) Pull-out specimen subjected to 67 kN, (b) Full-field major principal strain distribution, e_1, (c) Full-field minor principal strain distribution, e_2 and (d) Full-field principal strain angle (in radians)

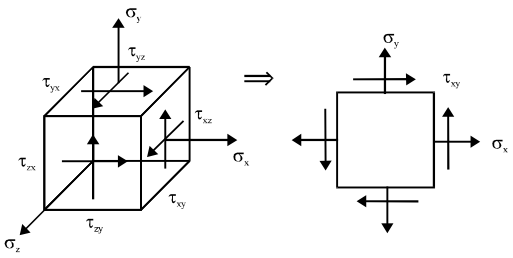

Fig. 7: Plain stress descriptions

is more than top of the bar on the surface of the specimen. In other words, these two mentioned area have opposite rotation angle on the plane of specimen due to subjected tensile force.

Stress distribution: One step further, after obtaining the result of correlation analysis, is calculation of the related bond stress. Considering the face of specimen as plane stress ($\sigma_{iz} = 0$), we can simplify the components as shown in Fig. 7.

From advanced mechanics of material we have Eq. 1 for calculating stresses in plain stress based on strains (e), young module (E) and Poisson ratio (v).

$$\begin{bmatrix}\sigma_x\\ \sigma_y\\ \tau_{xy}\end{bmatrix} = \frac{E}{1-\nu^2}\begin{bmatrix}1 & \nu & 0\\ \nu & 1 & 0\\ 0 & 0 & \frac{1}{2}(1-\nu)\end{bmatrix}\begin{bmatrix}e_x\\ e_y\\ 2e_{xy}\end{bmatrix} \quad (1)$$

Substitution of (E) and (v) by their values the above Eq. 1 simplified as in Eq. 2:

$$\begin{bmatrix}\sigma_x\\ \sigma_y\\ \tau_{xy}\end{bmatrix} = 27395.83\begin{bmatrix}1 & .2 & 0\\ .2 & 1 & 0\\ 0 & 0 & .8\end{bmatrix}\begin{bmatrix}e_x\\ e_y\\ e_{xy}\end{bmatrix} \quad (2)$$

With having this equation and the strains from DIC analysis, three components of stress can be calculated for every point of specimen. Thanks to Excel that eases these considerable operations along remarkable plots just by doing some table work. Three full-field stress distributions are calculated and drawn for normal stresses and shear stress on the face of specimen in Fig. 8.

Considering the drawn full-field stress distribution plots, the trace of the bar is observed clearly on the surface of specimen, due to existence of the bond. Ferguson *et al.* (1988) also presented the stress

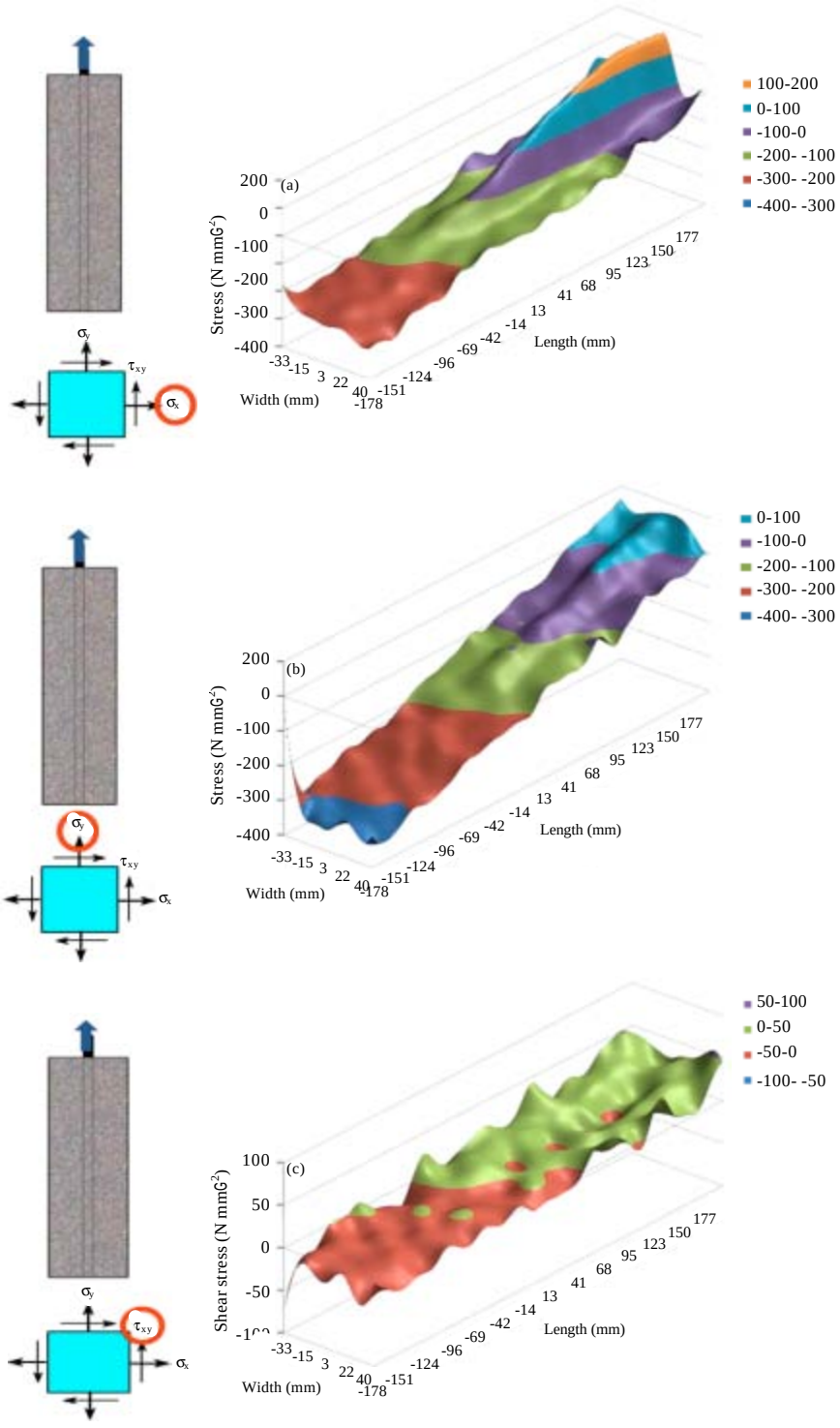

Fig. 8(a-c): Normal full-field stress distribution of specimen in 67 kN, (a) Normal stress σ_x (N mm^{-2}), (b) Normal stress σ_y (N mm^{-2}) and (c) Shear stress τ_{xy} (N mm^{-2})

distribution in 1988 as shown in Fig. 9 by different method. Comparing this figure with the calculated stress distribution in Fig. 8a, the high similarity can be found easily in the shape and trend of stress changes at the both figures. However, the full-field stress distribution obtained by DIC results (Fig. 8a) gives more detail information about the bond behavior and it seems more suitable than the other methods for investigation on the bond field.

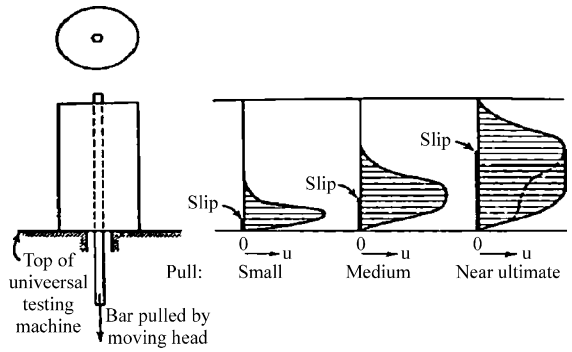

Fig. 9: Bond stress distribution (Ferguson *et al*., 1988)

In order to have accurate evaluation of stress growth throughout loading process two perpendicular lines on critical area of specimen are selected and the variations of stress is mapped versus tensile load rising. Figure 10 illustrates the changes of normal stress in x direction on a line (y = 100 mm) in the width of the specimen, by growing tensile load till failure. The first curve of this figure shows the changes of σ_{xx}, when load is 12 kN. As it can be seen, the whole stresses have minus amount which shows the area is on pressure in this stage. By load increasing, the line shape of curve converts to polynomial because of the bond effect. In other words, the bond changes the surface elements behavior in the vicinity of the bar by changing their stress sign from negative to positive or from compression to tension.

The following chart, Fig. 11, illustrates the changes of normal stress in x direction on a line (x = 0) in the length of

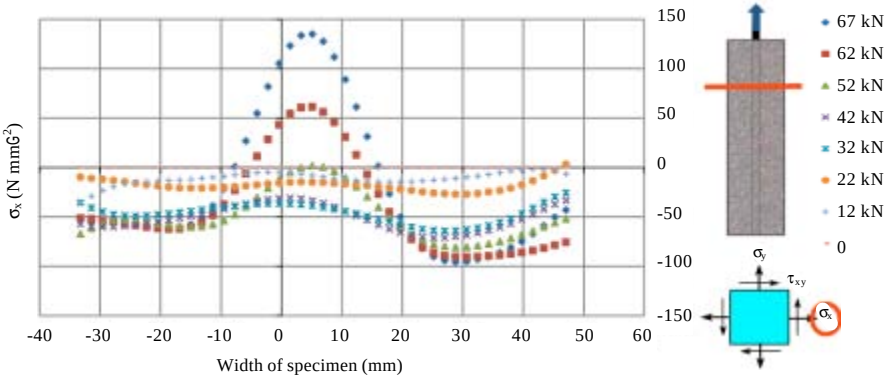

Fig. 10: Normal stress (σ_x) on the transversal surface line (y = 10) in various tensile forces

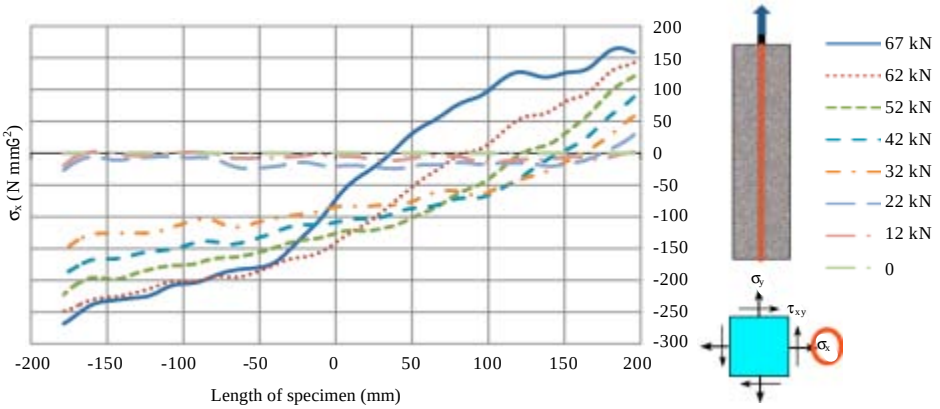

Fig. 11: Normal stress (σ_x) on the longitudinal surface line (x = 0) in various tensile forces

the specimen by growing tensile load till failure. In this chart, at two initial loads, there is uniform increasing in σ_x at entire line except in the top that is related to reaction of the support. The σ_x of the bottom part has a high decrease in stress that it may connect to unwilling out of plane motion of the end of specimen. The shape of increasing of the stresses in top of the specimen shows the effect of the bond in stresses on the surface. These stresses have positive sign in the last loads and can be considered as tension stresses. It seems that this bond stress component cause extensive tension on elements more than strength of concrete and can be known as a generating factor of crack and failure of specimen in the end.

Moreover from Fig. 11, the distribution of bar tension is predictable in the length of specimen. Since, this tension magnitude in each unit length of the bar is equal to sum of the related bond stress in around of the bar in concrete, so the shape of tension distribution follows the shape of bond stress in concrete. This claim is supported by the result of the experimental work that was carried out by Feldman and Michael Bartlett (2007) about bond stress along bar in pullout specimen. The other outcome of that investigation is about the peak bond stress shifting from loaded end to unloaded end of specimen during the increase of applied load, the behavior which is clearly observed from figures in Fig. 11. Likewise, the development of bond stress distribution under load increment conforms to the result of finite element analysis for bonding simulation in the research work with similar condition which was accomplished by Chen and Pan (2006).

CONCLUSION

A full-field measuring system based on digital image correlation was successfully applied to measure non-uniform strain of bond on the surface of concrete pull-out specimen, subjected to tensile force. It was presented that this method is a robust tool that has many benefits regarding to the testing conditions. Moreover, it was showed that the bond stress can be calculated numerically by using the results of 2D DIC. The development of non-uniform bond strain and stress in concrete was depicted with full-field distribution maps, plus the growth of bond stress at various loading stages. Considering the presented figures, it is deduced that the proposed numerical method for calculation of bond stress in concrete using 2D DIC results has adequate capability to investigate bond stress in concrete precisely.

ACKNOWLEDGMENTS

The author thanks the Universiti Teknologi Malaysia (UTM) and its Structural and Material Lab for supporting of this research work. Also, the author is grateful to Dr. Redzuan Abdullah for the valuable guidelines and useful comments to complete this research.

REFERENCES

Bing, P., X. Hui-min, X. Bo-qin and D. Fu-long, 2006. Performance of sub-pixel registration algorithms in digital image correlation. Meas. Sci. Technol., 17: 1615-1621.

Chen, J.F. and W.K. Pan, 2006. Three dimensional stress distribution in FRP-to-concrete bond test specimens. Constr. Build. Mater., 20: 46-58.

Feldman, L.R. and F. Michael Bartlett, 2007. Bond stresses along plain steel reinforcing bars in pullout specimens. Structural J., 104: 985-992.

Ferguson, P.M., J.E. Breen and J.O. Jirsa, 1988. Reinforced Concrete Fundamentals. 5th Edn., John Wiley and Sons, New York.

Haddadi, H. and S. Belhabib, 2008. Use of rigid-body motion for the investigation and estimation of the measurement errors related to digital image correlation technique. Opt. Lasers Eng., 46: 185-196.

Herbert, D.M., D.R. Gardner, M. Harbottle, J. Thomas and T.G. Hughes, 2011. The development of a new method for testing the lateral load capacity of small-scale masonry walls using a centrifuge and digital image correlation. Constr. Build. Mater., 25: 4465-4476.

Knauss, W.G., I. Chasiotis and Y. Huang, 2003. Mechanical measurements at the micron and nanometer scales. Mech. Mater., 35: 217-231.

Nadim Hasson, M. and A. Al-Manaseer, 2008. Structural Concrete Theory and Design. John Wiley, New Jersey.

Pan, B. and H.M. Xie, 2009. Assessment and correction of lens distortion for digital image correlation. Acta. Metro. Sin., 30: 62-67.

Pan, B., A. Asundi, H. Xie and J. Gao, 2009a. Digital image correlation using iterative least squares and pointwise least squares for displacement field and strain field measurements. Opt. Lasers Eng., 47: 865-874.

Pan, B., K. Qian, H. Xie and A. Asundi, 2009b. Two-dimensional image correlation for in-plane displacement and strain measurement: A review. Meas. Sci. Technol. Vol. 20.

Peter, W.H. and W.F. Ranson, 1982. Digital imaging technique in experimental stress analysis. Opt. Eng., 21: 427-431.

Rouchier, S., 2012. Characterization of fracture patterns and hydric properties for moisture flow modeling in cracked concrete. Constr. Build. Mater., 34: 56-62.

Schreier, H.W., 2003. Investigation of two and three-dimensional image correlation techniques with applications in experimental mechanics. Ph.D. Thesis, University of South Carolina, USA.

Sutton, M.A., C. Mingqi, W.H. Peters, Y.J. Chao and S.R. McNeill, 1986. Application of an optimized digital correlation method to planar deformation analysis. Image Vision Comput., 4: 143-150.

Sutton, M.A., J.H. Yan, V. Tiwari, H.W. Schreier and J.J. Orteu, 2008. The effect of out-of-plane motion on 2D and 3D digital image correlation measurements. Opt. Lasers Eng., 46: 746-757.

Valenca, J., D. Dias-da-Costa and E.N.B.S. Julio, 2012. Characterization of concrete cracking during laboratorial tests using image processing. Constr. Build. Mater., 28: 607-615.

Vandewalle, L. and F. Mortelmans, 1988. The bond stress between reinforcement bar and concrete: Is theoretically predictable? Mater. Struct., 21: 179-181.

Vidya Sagar, R. and B.K. Raghu Prasad, 2012. Damage limit states of reinforced concrete beams subjected to incremental cyclic loading using relaxation ration analysis of AE parameters. Constr. Build. Mater., 35: 139-148.

William, H.P., 2003. C++ Numerical Algorithms. Publishing House of Electronics Industry, Beijing, China.